1521-0111/92/3/327–337$25.00
MOLECULAR PHARMACOLOGY

https://doi.org/10.1124/mol.116.106880
Mol Pharmacol 92:327–337, September 2017

The $(\alpha4)_3(\beta2)_2$ Stoichiometry of the Nicotinic Acetylcholine Receptor Predominates in the Rat Motor Cortex[S]

Kristen E. DeDominicis, Niaz Sahibzada, Thao T. Olson, Yingxian Xiao, Barry B. Wolfe, Kenneth J. Kellar, and Robert P. Yasuda

Department of Pharmacology and Physiology, Georgetown University School of Medicine, Washington, DC

Received September 12, 2016; accepted July 6, 2017

ABSTRACT

The $\alpha4\beta2$ nicotinic acetylcholine receptor (nAChR) is important in central nervous system physiology and in mediating several of the pharmacological effects of nicotine on cognition, attention, and affective states. It is also the likely receptor that mediates nicotine addiction. This receptor assembles in two distinct stoichiometries: $(\alpha4)_2(\beta2)_3$ and $(\alpha4)_3(\beta2)_2$, which are referred to as high-sensitivity (HS) and low-sensitivity (LS) nAChRs, respectively, based on a difference in the potency of acetylcholine to activate them. The physiologic and pharmacological differences between these two receptor subtypes have been described in heterologous expression systems. However, the presence of each stoichiometry in native tissue currently remains unknown. In this study, different ratios of rat $\alpha4$ and $\beta2$ subunit cDNA were transfected into human embryonic kidney 293 cells to create a novel model system of HS and LS $\alpha4\beta2$ nAChRs expressed in a mammalian cell line. The HS and LS nAChRs were characterized through pharmacological and biochemical methods. Isolation of surface proteins revealed higher amounts of $\alpha4$ or $\beta2$ subunits in the LS or HS nAChR populations, respectively. In addition, sazetidine-A displayed different efficacies in activating these two receptor stoichiometries. Using this model system, a neurophysiological "two-concentration" acetylcholine or carbachol paradigm was developed and validated to determine $\alpha4/\beta2$ subunit stoichiometry. This paradigm was then used in layers I–IV of slices of the rat motor cortex to determine the percent contribution of HS and LS $\alpha4\beta2$ receptors in this brain region. We report that the majority of $\alpha4\beta2$ nAChRs in this brain region possess a stoichiometry of the $(\alpha4)_3(\beta2)_2$ LS subtype.

Introduction

Neuronal nicotinic acetylcholine receptors (nAChRs) are pentameric ligand-gated cation channels composed of different combinations of α ($\alpha2$–$\alpha10$) and β ($\beta2$–$\beta4$) subunits. Different combinations of subunits define nAChR subtypes and confer distinguishing biophysical and pharmacological characteristics to the receptor. The $\alpha4\beta2$ nAChRs are the predominant heteromeric nAChRs in the mammalian brain (Whiting and Lindstrom, 1987; Flores et al., 1992; Mao et al., 2008) and are thought to mediate important physiologic actions of acetylcholine (ACh) and pharmacological effects of nicotine related to attention and cognition (Picciotto et al., 1995; Guillem et al., 2011; Lozada et al., 2012; Paolone et al., 2013; Oda et al., 2014) and affective states (Mineur and Picciotto, 2010; Turner et al., 2010; Anderson and Brunzell, 2012, 2015; Hussmann et al., 2014). In addition to their roles in normal central nervous system physiology, considerable evidence points to the involvement of these receptors in nicotine addiction and dependence (Marks et al., 1983; Schwartz and Kellar, 1983; Benwell et al., 1988; Flores et al., 1992, 1997; Perry et al., 1999; Staley et al., 2006; Wüllner et al., 2008; Marks et al., 2011). Because of the wide-ranging role these receptors play in the central nervous system, understanding their structure in native tissue is particularly important.

Although $\alpha4\beta2$ nAChRs may include additional subunits, such as $\alpha4\beta2\alpha5$ (Mao et al., 2008), the simpler receptor complex composed only of $\alpha4$ and $\beta2$ subunits appears to predominate in most rat brain regions (Perry et al., 2007; Mao et al., 2008). Early work with chick $\alpha4\beta2$ nAChRs heterologously expressed in oocytes suggested that these receptors adopted a stoichiometry of $(\alpha4)_2(\beta2)_3$ (Anand et al., 1991). However, subsequent experiments that altered the proportion of $\alpha4$ and $\beta2$ subunits expressed in oocytes by injecting different amounts of subunit cDNA demonstrated that $\alpha4\beta2$ nAChRs can form with two distinct stoichiometries in heterologous expression systems (Zwart and Vijverberg, 1998; Nelson et al., 2003). The $(\alpha4)_2(\beta2)_3$ and $(\alpha4)_3(\beta2)_2$ nAChRs have been called high-sensitivity (HS) and low-sensitivity (LS) receptors, respectively, based on the potency of ACh to activate these receptor subtypes (Moroni et al., 2006).

In addition to their different sensitivities to ACh, other important differences between HS and LS $\alpha4\beta2$ nAChRs have been observed, including: 1) different potencies and efficacies

This work was supported by the National Institutes of Health National Institute on Drug Abuse [Grants R01-DA012976 and U19-DA027990].
https://doi.org/10.1124/mol.116.106880.
[S] This article has supplemental material available at molpharm.aspetjournals.org.

ABBREVIATIONS: 95% CI, 95% confidence interval; A85380, 3-[(2*S*)-2-azetidinylmethoxy]-pyridine dihydrochloride; ACh, acetylcholine; ACSF, artificial cerebrospinal fluid; CARB, carbachol; DHβE, dihydro-β-erythroidine; HEK293, human embryonic kidney 293; HS, high sensitivity; ISI, interstimulus interval; LS, low sensitivity; MLA, methyllycaconitine; nAChR, nicotinic acetylcholine receptor; PBS, phosphate-buffered saline; Saz-A, sazetidines-A; TEE, Tris, EDTA, and EGTA.

of nicotine and sazetidine-A (Saz-A) (Moroni et al., 2006; Zwart et al., 2008; Carbone et al., 2009), and 2) differences in calcium conductance through the channel, with the LS receptor passing more calcium than the HS receptor (Tapia et al., 2007). Furthermore, single-channel recordings in heterologously-expressed $\alpha4\beta2$ nAChRs indicate high and low conductance states which might be attributable to HS and LS receptors. However, no consensus has been reached as to which stoichiometry corresponds to which conductance level (Buisson and Bertrand, 2001; Nelson et al., 2003). Indeed, a recent study revealed a low conductance channel (29 pS) corresponding to the HS receptor and a high conductance channel (44 pS) corresponding to the LS receptor (Carignano et al., 2016). Interestingly, in addition to the receptor's canonical orthosteric agonist binding site at the $\alpha4/\beta2$ interface, it appears that activation of an $\alpha4/\alpha4$ binding site, which is present only in the LS nAChR that possesses the $(\alpha4)_3(\beta2)_2$ stoichiometry (Harpsøe et al., 2011; Mazzaferro et al., 2011; Wang et al., 2015), contributes to some of the differences between HS and LS receptor subtypes, including greater efficacy of some agonists (Harpsøe et al., 2011; Wang et al., 2015) and decreased desensitization (Benallegue et al., 2013; Eaton et al., 2014).

Although both stoichiometries of the $\alpha4\beta2$ nAChR assemble in heterologous expression systems, their presence in native tissue is not known with certainty. Some evidence suggests that both subtypes may assemble in the brain. For example, previous studies have demonstrated that mouse brain synaptosomes have a biphasic response to ACh with an HS and LS component, each phase of which is substantially reduced upon knockout of the $\alpha4$ or $\beta2$ subunits (Marks et al., 1999, 2007).

We present here a model of nonlinked HS and LS rat $\alpha4\beta2$ nAChRs expressed in mammalian cells. Using this model, we propose a method that exploits the differences in sensitivity between the two stoichiometric isoforms of the receptor to determine the contribution of HS or LS nAChR subtypes in the rat motor cortex. We report that a majority of $\alpha4\beta2$ nAChRs found in the rat motor cortex exhibit a response to ACh that is indicative of the LS $(\alpha4)_3(\beta2)_2$ nAChRs.

Materials and Methods

Materials. Human embryonic kidney 293 (HEK293) cells, Dulbecco's modified Eagle's medium, Lipofectamine, and Plus Reagent were purchased from Thermo Fisher Scientific (Waltham, MA). Primary antibodies against the nAChR $\alpha4$ subunit (sc-1772) or the nAChR $\beta2$ subunit (sc-11372) were purchased from Santa Cruz Biotechnology (Dallas, TX). Polyclonal antibodies against the nAChR $\alpha3$ and $\alpha5$ subunits were produced as described previously (Yeh et al., 2001; Lomazzo et al., 2011). Carbachol (CARB; carbamylcholine chloride), atropine sulfate, ACh chloride, dihydro-β-erythroidine (DHβE), Thesit, phosphatidylcholine, poly(D-lysine), and primary antibodies against β-actin (A5316), the nAChR $\beta2$ subunit (mAb290), and the nAChR $\alpha4$ (mAb299) were purchased from Sigma-Aldrich (St. Louis, MO). Secondary antibodies (800CW 926-32214 and 680LT 926-68023) and blocking buffer were purchased from LI-COR Biosciences (Lincoln, NE). NeutrAvidin agarose resin, Protein G Ultralink, and EZ-Link Sulfo-NHS-LC-LC-Biotin were purchased from Thermo Fisher Scientific. Saz-A was obtained from RTI International (Research Triangle Park, NC). Methyllycaconitine (MLA) was supplied by the National Institutes of Health National Institute on Drug Abuse (Bethesda, MD).

Cell Culture and Transfection. HEK293 cells were cultured in Dulbecco's modified Eagle's medium with 10% fetal bovine serum. Cells were plated and transiently transfected with rat $\alpha4$ and $\beta2$ nAChR subunit cDNA using Lipofectamine and the Plus Reagent. Cells used for biotinylation experiments were plated in 100-mm dishes to approximately 90% confluence and were transfected the following day with $\alpha4$ and $\beta2$ nAChR subunit cDNA in a molar ratio of 1:6 or 4:1 $\alpha4/\beta2$ to generate HS or LS $\alpha4\beta2$ nAChRs, respectively. The rat $\alpha4$ and $\beta2$ nAChR subunit plasmid cDNA construction was described previously (Xiao and Kellar, 2004). Cells used for electrophysiology recording experiments were plated at low density on poly(D-lysine)–coated coverslips using a flame-polished pipette. The next day, these cells were cotransfected with green fluorescent protein and ($\alpha4$ plus $\beta2$) subunit cDNA in a molar ratio of 1:4 green fluorescent protein/($\alpha4$ plus $\beta2$), in which the relative molar ratios of $\alpha4$ and $\beta2$ subunit cDNA were 1:6 (HS $\alpha4\beta2$ nAChR) or 4:1 (LS $\alpha4\beta2$ nAChR). To upregulate receptors for both biotinylation and electrophysiology experiments, the HS $\alpha4\beta2$ nAChRs were cultured in the presence of 1 mM CARB plus 10 μM atropine, whereas the LS $\alpha4\beta2$ nAChRs were cultured in the presence of 1 mM CARB.

Cell Surface Labeling. Surface proteins of transfected HEK293 cells were biotinylated 24 hours after transfection. Cells were washed three times with phosphate-buffered saline (PBS) buffer (1.1 mM potassium phosphate monobasic, 155 mM sodium chloride, and 3 mM sodium phosphate dibasic, pH 8; 37°C) and were then incubated in Versene (37°C) and gently transferred to 15-ml conical tubes. Cells were spun at approximately 500*g* and were gently resuspended in ice-cold PBS and then placed on ice. The biotinylating reagent (EZ-Link Sulfo-NHS-LC-LC-Biotin) at a final concentration of 1.7 mM was added to the cell suspension and incubated for 20 minutes on ice with gentle rotation. The reaction was quenched with three washes of 100 mM glycine. Cell membrane homogenates were isolated by sonication in Tris, EDTA, and EGTA (TEE) buffer (10 mM Tris, 5 mM EDTA, and 5 mM EGTA, pH 7.4) and centrifuged at 30,000*g* at 4°C for 15 minutes. The membrane pellet was resuspended in TEE buffer.

Isolation of Biotin-Labeled Cell Surface Proteins and Immunoprecipitation. Biotin-labeled HEK293 membrane homogenates were solubilized in TEE buffer containing 1% Thesit, 1.8 mM phosphatidylcholine, and 0.05% SDS for 4–6 hours at 2–8°C with gentle rotation. Cortical brain tissue homogenates were solubilized in TEE buffer containing 2% Triton-X, 1.8 mM phosphatidylcholine, and 0.05% SDS for 4–6 hours at 2–8°C with gentle rotation. Samples were then centrifuged at 30,000*g* for 30 minutes at 4°C to pellet the membrane fraction. Solubilized proteins in the supernatant were added to NeutrAvidin agarose resin or mAb299 ($\alpha4$ selective) or mAb290 ($\beta2$ selective) antibodies covalently coupled to Protein G resin as described previously (Hussmann et al., 2014). Samples were then mixed and were incubated at 2–8°C with gentle rotation overnight. NeutrAvidin-biotin complexes and immunoprecipitations were pelleted at 1000*g* and washed three times with 1% Thesit in TEE buffer. The final pellet was suspended in Laemmli loading buffer (Laemmli, 1970) for subsequent analysis by Western blot.

Western Blots. Denatured protein samples were separated by SDS-PAGE on 9% polyacrylamide gels. Proteins were transferred to polyvinylidene fluoride membranes with low background fluorescence (LI-COR Biosciences) and then blocked using the LI-COR Odyssey blocking buffer diluted 2× with PBS. Blocked membranes were probed with primary antibodies against the $\alpha4$ nAChR subunit (1 μg/ml), $\beta2$ nAChR subunit (1 μg/ml), $\alpha3$ nAChR subunit (1 μg/ml), $\alpha5$ nAChR subunit (1 μg/ml), or β-actin (1:5000) and followed with secondary antibodies. All membranes were imaged using the Odyssey Infrared Imaging System (LI-COR Biosciences). Bands for the $\alpha4$ and $\beta2$ subunits were imaged simultaneously from the same sample lane on a single membrane using dual color detection. Bands for β-actin were visualized on separate membranes. The $\alpha3$ and $\alpha5$ nAChR subunits were visualized on membranes containing controls with either stably transfected rat $\alpha4\beta2$ nAChRs or rat $\alpha3\beta4$ nAChRs and transiently transfected rat $\alpha4\beta2\alpha5$ nAChRs in HEK cells.

Preparation of Brain Slices. Brain slices were obtained from P16–P24 male Sprague-Dawley rat pups. Animals were quickly decapitated and the brains were removed and transferred to ice-cold artificial cerebrospinal fluid (ACSF) containing the following: 121 mM NaCl, 2.5 mM KCl, 2 mM $CaCl_2$, 1 mM $MgCl_2$, 1.25 mM NaH_2PO_4, 26 mM $NaHCO_3$, 10 mM glucose,

5 mM HEPES, and 3 mM myoinositol, which was continuously oxygenated with 95% O_2 plus 5% CO_2. Coronal brain slices (250 μm) were cut from the motor cortex region (approximately 2.2 mm to the bregma) using a vibratome (Leica VT1000S, Leica Biosystems, Buffalo Grove, IL) and were incubated for 30 minutes at 37°C in oxygenated ACSF followed by 30 minutes at room temperature (21°C) until used for recording. All procedures were performed according to the National Institutes of Health guidelines for the ethical use of animals in research and were approved by the Georgetown University Animal Care and Use Committee.

Preparation of HEK293 Cells for Electrophysiology Experiments. Transiently transfected HEK293 cells expressing $\alpha4\beta2$ nAChRs were used in experiments 24 hours post-transfection. Coverslips were washed six times in fresh culture media to remove upregulating agents and were then incubated for at least 1 hour at 37°C until use. The extracellular solution for recording consisted of 130 mM NaCl, 5 mM KCl, 2 mM $CaCl_2$, 2 mM $MgCl_2$, 10 mM glucose, and 10 mM HEPES, pH 7.4.

Electrophysiology Experiments. Coverslips containing transfected $\alpha4\beta2$ HEK293 cells or brain slices from the motor cortex were transferred to a recording chamber (500 μl volume) attached to the stage of a Nikon E600-FN microscope (Nikon Instruments, Melville, NY), where they were continuously perfused with the appropriate extracellular ACSF solutions listed above. The ACSF solutions were corrected for osmolarity to approximately 296 mOsm/l.

Recordings were made with patch electrodes (4–6 MΩ) pulled from borosilicate glass and filled with an internal recording solution containing 145 mM K gluconate, 5 mM EGTA, 2.5 mM $MgCl_2$, 10 mM HEPES, 5 mM ATP•Na, and 0.2 mM GTP•Na, pH 7.2, adjusted to 285 mOsm/l. Cells were identified visually by infrared-differential interference contrast and fluorescence optics via a charge-coupled device camera (DAGE S-75, DAGE-MTI, Michigan City, IN). A 60× water immersion objective (Nikon Instruments) was used to approach cells and neurons. Whole-cell voltage clamp recordings of HEK293 cells and neurons (V_{hold} = −60 mV) were obtained using a MultiClamp 700B (Molecular Devices, Sunnyvale, CA). Signals, acquired at 20 kHz, were low-pass filtered at 2 kHz, digitized (Digidata 1440A; Molecular Devices), and stored on a personal computer for subsequent analysis. Prior to recording agonist-induced whole-cell currents, pipette and cell capacitance was minimized and series resistance (<12 MΩ) was compensated via MultiClamp Commander software (Molecular Devices). Input and access resistances were monitored by a 5-mV hyperpolarization pulse throughout the recording session.

Drug Solutions and Application. Ligands for application during electrophysiology experiments (ACh, CARB, Saz-A, DHβE, MLA) were prepared in extracellular solutions (i.e., for HEK293 cells or brain slices). Atropine (1 μM) was added to all drug solutions to block possible long-term effects from activation of muscarinic receptors.

For ACh concentration-response curves and Saz-A experiments, agonists were applied by a "y-tubing" positioned above the recording cell. For experiments examining the response to 10 and 1000 μM ACh or 32 and 1000 μM CARB, agonists were applied by two borosilicate glass pipettes located approximately 5–20 μm from the cell body using a picospritzer (one pipette for each concentration). In HEK293 cells at concentrations of ACh or CARB ≤32 μM, an interstimulus interval (ISI) of at least 5 minutes was necessary to allow receptors to recover from desensitization, whereas an ISI of 10 minutes was required for ACh or CARB concentrations >32 μM. In brain-slice experiments, a 5-minute ISI was sufficient to allow receptors to recover from desensitization between subsequent applications with ACh.

Antagonists (MLA and DHβE) were applied via bath application. The concentration of 10 nM MLA was chosen because it is routinely used in the literature to block responses from α7 nAChRs (Christophe et al., 2002; Sahibzada et al., 2002; Xiao et al., 2009; Alves et al., 2010). In some experiments, MLA 10 nM was directly added to the ACSF that contained 1 μM atropine. A concentration of 10 μM DHβE was used to inhibit both HS and LS $\alpha4\beta2$ nAChRs (Moroni et al., 2006).

Data Analysis. All data are presented as means ± S.E. Quantification for electrophysiology experiments was based on peak amplitude values, which were obtained using Clampfit 10.2 software (Molecular Devices). Concentration-response curves were fit using the following GraphPad Prism 5 (GraphPad Software Inc., La Jolla, CA) equation: "log(agonist) versus response − Variable slope (four parameters)." The reported EC_{50} values were calculated from this equation. Differences between the HS and LS $\alpha4\beta2$ nAChRs were compared statistically with an unpaired t test. A value of $P < 0.05$ was considered significant.

Results

Altering Transfection Ratios of α4 and β2 Subunit cDNA into HEK293 Cells Favors Incorporation of More α4 or β2 Subunit Proteins at the Cell Surface. Altering injection ratios of α4 and β2 subunit cDNA or cRNA into *Xenopus laevis* oocytes produces either HS or LS nAChRs (Moroni et al., 2006; Harpsøe et al., 2011). We hypothesized that altering transfection ratios of α4 and β2 subunit cDNA into HEK293 cells would do the same. We initially biotinylated surface proteins

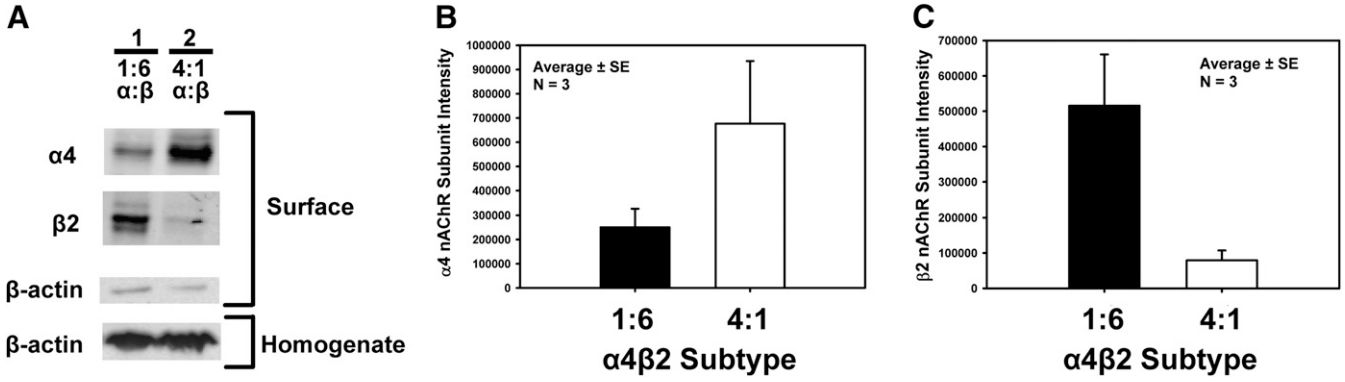

Fig. 1. Western blots of the 1:6 and 4:1 $\alpha4/\beta2$ transfection ratios in HEK293 cells demonstrate a shift in the relative amount of surface α4 and β2 subunit protein at the cell surface. Surface proteins were labeled by biotin and isolated with NeutrAvidin. Western blots were used to determine the presence of the α4 nAChR subunit, the β2 nAChR subunit, and β-actin proteins at the outside cell surface. (A) Lanes 1 and 2 show the surface α4 nAChR and β2 nAChR subunit proteins when transfected with $\alpha4/\beta2$ cDNA at 4:1 and 1:6 ratios, respectively. β-actin (surface) is used to determine the integrity of the cell membrane. β-actin (homogenate) acts as an internal control to confirm isolation of surface proteins only. The banding pattern shown here is representative of four different transfections and surface labeling experiments in which both transfection ratios were assessed. (B and C) Quantification of the α4 nAChR subunit protein (B) and the β2 nAChR subunit protein (C) in 1:6 (black) and 4:1 (white) $\alpha4/\beta2$ transfection ratios is presented. Each bar represents three different transfections and surface labeling experiments in which both transfection ratios were assessed. Please note that the number of samples for (B) and (C) has dropped from four to three [as compared with (A)] because one experiment used a different secondary antibody dilution and is therefore not included.

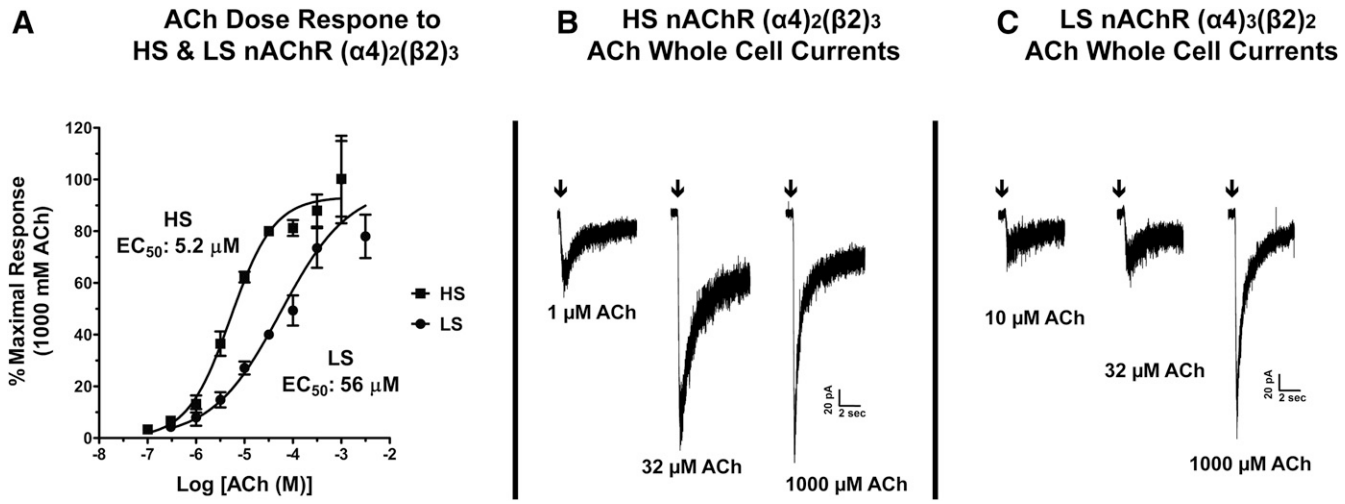

Fig. 2. Alternate transfection ratios of rat $\alpha 4/\beta 2$ cDNA into HEK293 cells favor assembly of HS or LS $\alpha 4\beta 2$ nAChRs. Rat $\alpha 4$ and $\beta 2$ cDNA were transfected in a molar ratio of 1:6 (HS) or 4:1 (LS) $\alpha 4/\beta 2$ cDNA. (A) Concentration-response curves to ACh were obtained using whole-cell voltage clamp electrophysiology. Drugs were applied by y-tubing. The peak amplitude response from each ACh concentration was normalized to the response from 32 μM in the same cell. Values were first normalized and plotted against the 32 μM ACh response and were then replotted here for clarity as a percentage of the maximal 1000 μM response to highlight the difference in ACh sensitivity between the two ratios. Each data point represents values from two to three cells. No more than three ACh responses were obtained from each cell. Twenty and 24 cells were recorded from 11 or 13 different transfections to obtain data for the transfection of 1:6 and 4:1 molar ratios, respectively. Data were fit using a nonlinear regression model with variable slope. (B) Representative traces of ACh responses in HS $\alpha 4\beta 2$ nAChR from the same transfected cell. (C) Representative traces of ACh responses in LS $\alpha 4\beta 2$ nAChR from the same transfected cell. The ACh currents are from the data used to generate the dose-response curves in (A). The arrows denote when the y-tubing application of ACh was started.

to examine the relative proportion of $\alpha 4$ and $\beta 2$ subunit protein present at the cell surface after transfecting $\alpha 4$ and $\beta 2$ nAChR subunit cDNA at molar ratios of 1:6 or 4:1 to create the HS $(\alpha 4)_2(\beta 2)_3$ or LS $(\alpha 4)_3(\beta 2)_2$ nAChR subtype, respectively. Isolating cell surface proteins is important because only receptors reaching the outside surface can mediate neurotransmitter signaling, thus allowing us to compare the subunit composition at the surface to function. As shown in Fig. 1A, altering the ratio

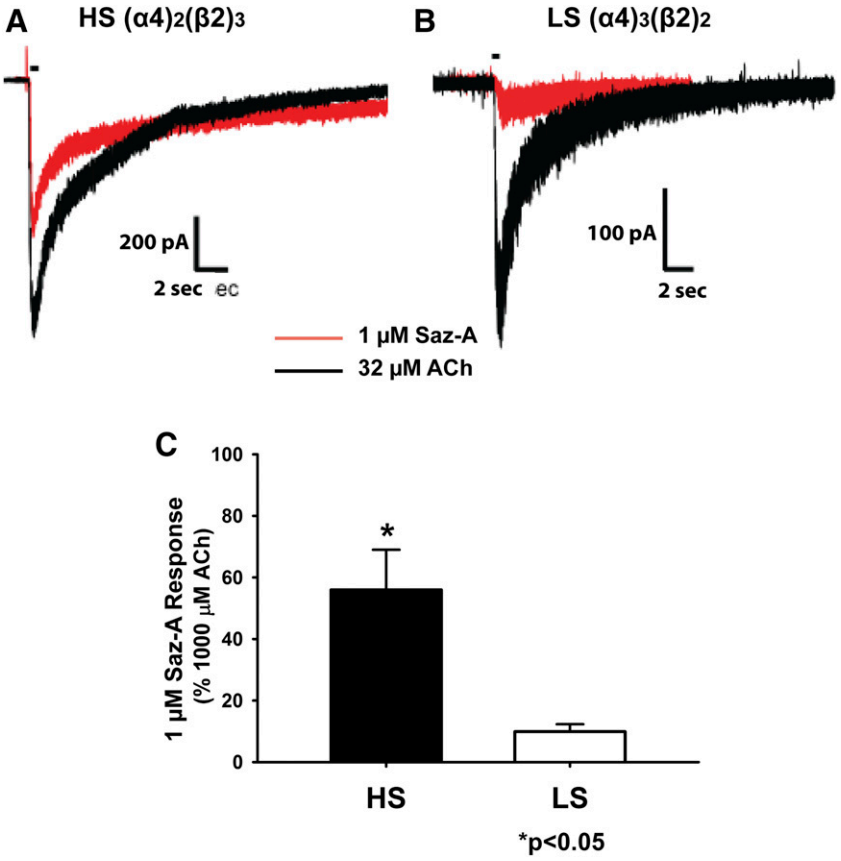

Fig. 3. Saz-A has greater potency at the HS $(\alpha 4)_2(\beta 2)_3$ than the LS $(\alpha 4)_3(\beta 2)_2$ nAChR in HEK293 cells, as determined by whole-cell voltage clamp electrophysiology. (A and B) Representative trace overlays of 1 μM Saz-A (red) and 32 μM ACh (black) are shown for the $\alpha 4/\beta 2$ cDNA transfections for HS $(\alpha 4)_2(\beta 2)_3$ (A) and LS $(\alpha 4)_3(\beta 2)_2$ (B). Drugs were applied using y-tubing. To avoid prolonged desensitization elicited by Saz-A in our experimental paradigm, 32 μM ACh was applied first, followed by the application of 1 μM Saz-A. (C) The average of the peak amplitude of the 1 μM Saz-A response normalized to the 1000 μM ACh response is shown for the $\alpha 4/\beta 2$ cDNA transfections for HS (black) and LS (white) nAChRs. $^*P < 0.05$ (t test, n = 4–6 cells from three to four different transfection days).

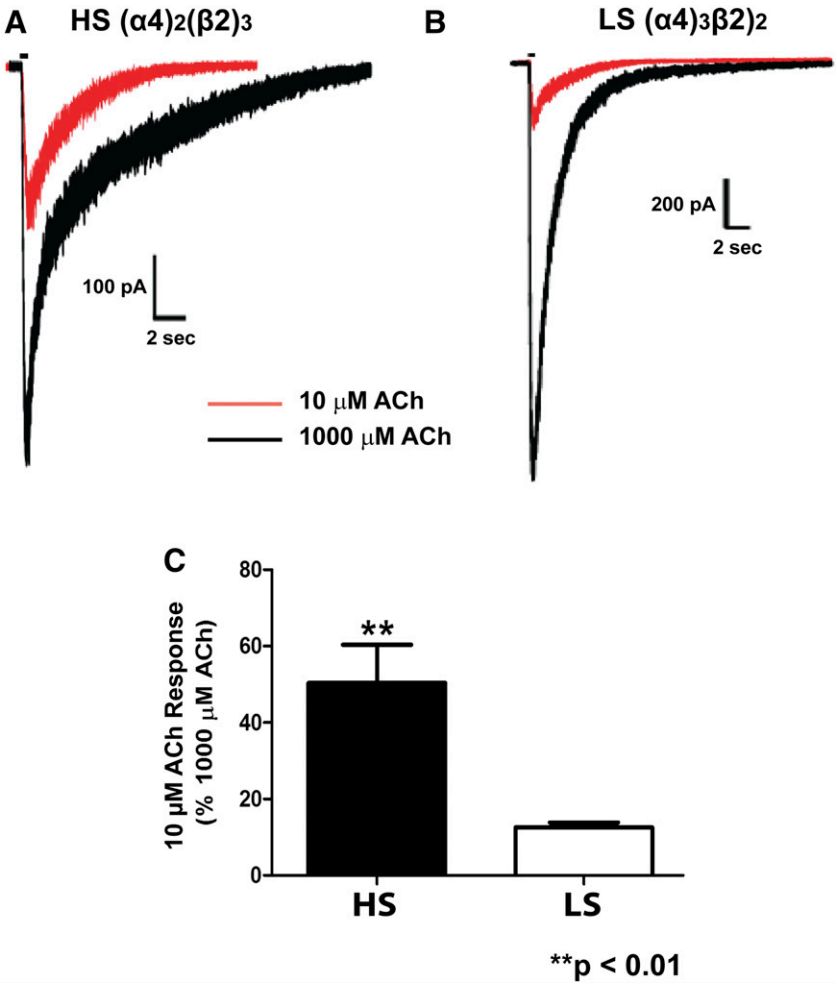

Fig. 4. Normalized 10 μM ACh responses demonstrate a stark difference in the HS $(\alpha4)_2(\beta2)_3$ and LS $(\alpha4)_3(\beta2)_2$ nAChRs in HEK293 cells as determined by whole-cell voltage clamp electrophysiology. (A and B) Representative trace overlays of 10 ACh (red) and 1000 μM ACh (black) are shown for the HS $(\alpha4)_2(\beta2)_3$ (A) and LS $(\alpha4)_3(\beta2)_2$ (B) nAChRs. Drugs were applied by pressure (picospritzer). (C) A compilation of the peak amplitude of the 10 μM ACh response normalized to the 1000 μM ACh response is shown for both transfection ratios. $^{**}P < 0.01$ (t test, $n = 9$ cells for each transfection ratio from two to three separate transfection days).

of $\alpha4$ and $\beta2$ subunit cDNA transfected into HEK293 cells results in a proportional shift of the $\alpha4$ and $\beta2$ subunit protein that reaches the cell surface. Figure 1, B and C, presents the quantification of the $\alpha4$ and $\beta2$ subunit band intensities, respectively, in the 1:6 and 4:1 transfection ratios of $\alpha4$ and $\beta2$ subunit cDNA. It is important to note that the intensities of the $\alpha4$ nAChR subunit protein and $\beta2$ nAChR subunit protein are not directly comparable, since each antibody is unique and different secondary antibodies are used for each subunit. Therefore, it is inappropriate to draw quantitative conclusions regarding receptor composition from these data alone. Western blot bands for β-actin (an intracellular protein) were present in membrane homogenates prior to surface protein isolation but were negligible in the surface-isolated fraction, which acts as an internal control for our experiment to confirm isolation of only surface-labeled proteins. It is important to note that the NeutrAvidin pull-down of the surface protein fraction is 16 times greater than the whole homogenate fraction (Fig. 1A); therefore, the trace of β-actin observed in the NeutrAvidin pull-down is nominal.

The Transfection Ratios Yield Receptors with Different ACh Sensitivity. As shown in Fig. 1, transfection ratios that favor more $\alpha4$ or $\beta2$ subunit cDNA result in receptors with more $\alpha4$ or $\beta2$ subunits, respectively, being assembled and reaching the cell surface. Next, we sought to assess whether these different $\alpha4/\beta2$ subunit ratios would functionally resemble HS or LS $\alpha4\beta2$ nAChRs as reported by others. Whole-cell voltage clamp ACh concentration-response curves were generated from rat $\alpha4\beta2$ nAChRs expressed in HEK293 cells transfected with $\alpha4/\beta2$ subunit cDNA ratios of 1:6 or 4:1. When cells with a transfection ratio of 1:6 $\alpha4/\beta2$ cDNA were used, the concentration-response relationship fit best to a single site that displayed a high sensitivity to ACh (Fig. 2A), with an EC_{50} of 5.2 μM [95% confidence interval (95% CI), 3.7–7.2 μM] and a Hill slope of 0.97 [95% CI, 0.74–1.19]. When cells with a transfection ratio of 4:1 of $\alpha4/\beta2$ cDNA were used, the concentration-response relationship also fit best to a single site but the sensitivity to ACh was 10-fold lower, with an EC_{50} of 56 μM (95% CI, 26–119 μM) and a Hill slope of 0.61 (95% CI, 0.41–0.81). Thus, the $\alpha4\beta2$ nAChRs assembled from these different transfection ratios demonstrate a clear shift in sensitivity to activation by ACh. Moreover, these EC_{50} values are similar to others that have been reported previously for the ACh high- and low-affinity nAChR sites for human $\alpha4\beta2$ stably expressed in HEK293 cells (Nelson et al., 2003) and for human HS $(\alpha4)_2(\beta2)_3$ or LS $(\alpha4)_3(\beta2)_2$ nAChR subtypes expressed in oocytes (Harpsøe et al., 2011). Representative traces of ACh gated currents for the HS and LS nAChRs are shown in Fig. 2, B and C.

Characterization of the HS and LS $\alpha4\beta2$ nAChR Subtypes Using Saz-A. Saz-A, a high-affinity ligand for $\alpha4\beta2$ nAChRs (Xiao et al., 2006), is a nearly full agonist at human HS $\alpha4\beta2$ nAChRs but a very weak partial agonist at human LS $\alpha4\beta2$

nAChRs (Zwart et al., 2008; Eaton et al., 2014). Here, we compared the efficacy of 1 μM Saz-A to 32 μM ACh at rat nAChRs in cells expressing the HS or LS $\alpha4\beta2$ nAChR subtype. We used a concentration of 1 μM Saz-A because it elicits a maximal response at both the human HS and LS $\alpha4\beta2$ nAChR subtypes, although the response at the LS receptors is only approximately 6% of that at the HS receptor (Zwart et al., 2008). A concentration of 32 μM ACh was used for comparison because it provided robust responses at both forms of the receptor without the prolonged recovery time necessary after activation with higher concentrations of ACh. The mean peak amplitude of whole-cell responses elicited by 1 μM Saz-A compared with 32 μM ACh was significantly different at the HS and LS nAChRs (Figs. 3, A and B, respectively). In cells that expressed the HS nAChR, Saz-A stimulated 69% ± 16% of the peak amplitude response elicited by 32 μM ACh, whereas it stimulated only 25% ± 6% of the ACh response in cells that expressed the LS nAChRs. By extrapolating the 32 μM ACh to 1000 μM ACh responses specific to the appropriate HS or LS subtype, Saz-A stimulated peak amplitude responses of 56% ± 13% (HS) or 10% ± 2.4% (LS) compared with 1000 μM ACh (Fig. 3C). These results are consistent with the relative response elicited by Saz-A at HS and LS human $\alpha4\beta2$ nAChRs (Zwart et al., 2008).

High and Low Concentrations of ACh Distinguish between the HS and LS nAChRs. To test how well ACh distinguishes between this model of HS and LS nAChRs, we measured the responses to 10 and 1000 μM ACh in cells after transfection with our two different ratios of $\alpha4$ and $\beta2$ subunits (Fig. 4). We selected these two concentrations of ACh because, as shown in Fig. 2A, 1000 μM ACh maximally activates both HS and LS receptors, whereas 10 μM maximizes the differences in responses to ACh observed in the HS and LS receptor subtypes.

Comparing the peak amplitude response of 10 μM ACh against 1000 μM ACh at each of our transfection ratios showed a statistically significant difference between the HS and LS models of nAChRs. In cells transfected to yield the HS $\alpha4\beta2$ nAChR subtype, the peak amplitude whole-cell current response to 10 μM ACh was 50% ± 10% of the response to 1000 μM ACh; in cells transfected to yield the LS $\alpha4\beta2$ nAChR subtype, the peak response to 10 μM ACh was only 13% ± 2% that of the 1000 μM ACh response (Fig. 4). Thus, based on the responses to Saz-A and to the higher and lower concentrations of ACh, transfection of cells with these ratios of $\alpha4$ and $\beta2$ subunits can reliably produce the HS and LS nAChR subtypes.

Assessing the Stoichiometry of $\alpha4\beta2$ nAChRs in the Rat Brain. The ratio of the 10 to 1000 μM ACh responses are different at HS and LS receptors as evidenced by data from our model of HS and LS rat $\alpha4\beta2$ nAChRs in transfected cells. We will use this same ACh ratio method to determine the contribution of the HS or LS receptors in layers I–IV of the rat motor cortex slice preparation. We chose this brain region because: 1) the motor cortex contains a high percentage of neurons that are responsive to nAChR agonists (Porter et al., 1999; Christophe et al., 2002); 2) more than 90% of the heteromeric nAChRs in the rat cerebral cortex are an $\alpha4\beta2$ nAChR subtype (Flores et al., 1992; Mao et al., 2008), although approximately 15%–20% of these also contain the $\alpha3$ or $\alpha5$ nAChR subunit (Mao et al., 2008); and 3) nAChR $\alpha5$ mRNA is restricted to cortical layer VI (Wada et al., 1990; Marks et al., 1992). Pharmacological investigation with galanthamine also supports the presence of $\alpha5$-containing nAChRs exclusively in cortical layer VI (Kassam et al., 2008; Poorthuis et al., 2013). Galanthamine potentiates the $\alpha4\beta2$ nAChR response when the $\alpha5$ nAChR subunit is present (Kuryatov et al., 2008).

To further determine whether $\alpha3$ or $\alpha5$ nAChR subunits may assemble with the $\alpha4\beta2$ nAChRs in the motor cortex, we performed immunoprecipitation experiments with solubilized motor cortex brain tissue with antibodies specific to the $\alpha4$ or $\beta2$ nAChR subunits, followed by subsequent Western blotting

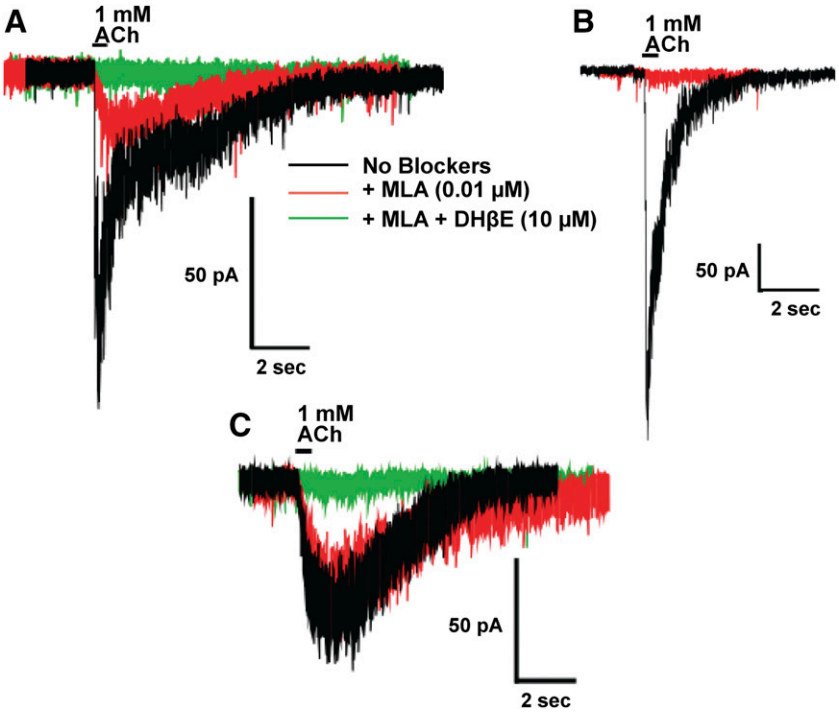

Fig. 5. Heterogeneity of nAChR responses in the rat motor cortex. (A–C) Four different types of nAChR responses were elicited by 1000 μM ACh in whole-cell patch-clamp electrophysiology recordings from neurons in layers I–IV of the motor cortex: nonresponsive neurons (data not shown), MLA-sensitive and DHβE-sensitive neurons (A), MLA-sensitive neurons (B), and MLA-insensitive and DHβE-sensitive neurons (C). Responses to 1000 μM ACh without blockers are shown in black. Responses elicited by 1000 μM ACh after 5-minute preincubation with 10 nM MLA are shown in red. Responses elicited by 1000 μM ACh after 5-minute preincubation with 10 μM DHBE and 10 nM MLA are shown in green.

experiments to assess the presence of $\alpha3$ and $\alpha5$ in isolated $\alpha4$ and $\beta2$ nAChR complexes. The $\alpha3$ subunit was not detectable after immunoprecipitation with either $\alpha4$ or $\beta2$ nAChR antibodies (Supplemental Fig. 1A), indicating that the coassembly of this subunit into $\alpha4\beta2$ nAChRs in this region is negligible. We did observe the coassembly of the $\alpha5$ nAChR subunit with $\alpha4\beta2$ nAChRs (Supplemental Fig. 1B) but, as mentioned previously, the $\alpha5$ subunit has been demonstrated to be confined to layer VI (Kassam et al., 2008; Poorthuis et al., 2013). Thus, cortical layers I–IV of the motor cortex provide an excellent brain region in which to study responses of $\alpha4\beta2$ nAChRs in isolation from other nAChR subunits.

To confirm this, we first assessed the nAChRs in layers I–IV of the motor cortex based on their responses to 1000 μM ACh and the sensitivity of those responses to blockade by the $\alpha7$ antagonist MLA and the $\alpha4\beta2$ antagonist DHβE. Although half of the neurons (18 of 36) were responsive to 1000 μM ACh, an equal number were unresponsive. In 78% of the responsive neurons (n = 14 of 18), 1000 μM ACh elicited a whole-cell current response composed of two components, one that was blocked by a 5-minute bath exposure to 10 nM MLA and a second component that was blocked upon a further 5-minute bath exposure to 10 μM DHβE (Fig. 5A), implying that these neurons expressed both $\alpha4\beta2$ and $\alpha7$ nAChRs. In 5% of the responsive neurons (n = 1 of 18), a 5-minute bath application of 10 nM MLA abolished whole-cell responses produced by 1000 μM ACh (Fig. 5B), which indicates that a small percentage of neurons in layers I–IV express $\alpha7$ nAChRs alone. In 17% of the neurons (n = 3 of 18), whole-cell currents elicited by 1000 μM ACh were completely inhibited by a 5-minute bath exposure of 10 μM DHβE (Fig. 5C), suggesting that these neurons express only $\alpha4\beta2$ nAChRs.

These data indicate that neurons in cortical layers I–IV contain nicotinic ACh–sensitive neurons that express either a mixture of $\alpha4\beta2$ and $\alpha7$ nAChRs, $\alpha4\beta2$ nAChRs alone, or $\alpha7$ nAChRs alone. Furthermore, within this population, neurons expressing a mixture of $\alpha4\beta2$ and $\alpha7$ nAChRs predominate. Thus, cortical layers I–IV of the motor cortex represent an appropriate region in which to measure responses from native $\alpha4\beta2$ nAChRs and to try to determine the stoichiometry of these receptors by utilizing our "two-concentration" ACh (10 and 1000 μM) whole-cell current activation paradigm.

Assessment of $\alpha4\beta2$ Stoichiometry by the Two-Concentration ACh Paradigm in the Motor Cortex. Since the majority of ACh-sensitive neurons in the motor cortex express a mixture of $\alpha4\beta2$ and $\alpha7$ nAChRs, all recordings were performed in the presence of the $\alpha7$ nAChR antagonist MLA (10 nM). This allowed us to assess the stoichiometry of $\alpha4\beta2$ nAChRs using the two-concentration ACh paradigm without a contribution from $\alpha7$ nAChRs. It should be noted that MLA did not decrease the peak amplitude of ACh currents elicited by the $\alpha4\beta2$ nAChRs expressed in the HEK293 cells. In addition, following the two-concentration ACh test paradigm, MLA-resistant responses from each recorded neuron were confirmed to result from activation of $\alpha4\beta2$ nAChRs by subsequent bath application of 10 μM DHβE, thus supporting the pharmacological isolation of $\alpha4\beta2$ nAChRs in our experiments. In this recording paradigm, the peak amplitude currents elicited by 10 μM ACh were 22% ± 3% of the currents elicited by 1000 μM ACh (Fig. 6). These results indicate that a majority of $\alpha4\beta2$ nAChRs in layers I–IV in the motor cortex have an LS subtype stoichiometry.

Assessment of $\alpha4\beta2$ Stoichiometry by a Two-Concentration CARB Paradigm in the Motor Cortex. To confirm this finding with a second cholinergic agonist and to demonstrate that endogenous acetylcholinesterase activity does not affect the ACh results presented here, we also applied a two-concentration CARB paradigm to our HEK HS (Fig. 7A) and LS (Fig. 7B) nAChRs and motor cortex recordings (Fig. 7C) using 32 and 1000 μM CARB. These data are quantified in Fig. 7D. CARB, a muscarinic and nicotinic ACh receptor agonist, is insensitive to cholinesterase activity (Brown and Laiken, 2011). Since the HEK cells and brain slices are bathed in 1 μM atropine in our experiments, CARB is only effective as a nAChR agonist under these conditions. These results look similar to those using a two-concentration ACh paradigm, further corroborating the stoichiometry of $\alpha4\beta2$ nAChRs in layers I–IV in the motor cortex is that of the LS subtype and indicating that cholinesterase activity does not affect the ACh paradigm presented here.

Biochemical Estimation of $\alpha4\beta2$ Stoichiometry in the Rat Cortex. To provide supporting biochemical evidence for the predominance of the LS $\alpha4\beta2$ nAChR stoichiometry in the motor cortex as determined by our patch-clamp electrophysiology recordings, we performed immunoprecipitation and Western blotting experiments. In these experiments, rat

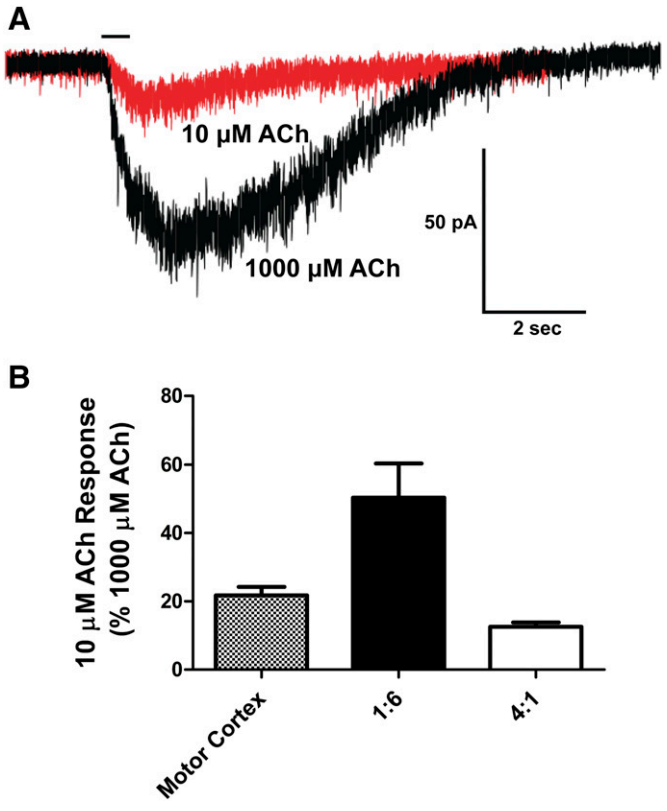

Fig. 6. Comparison of the responses to 10 and 1000 μM ACh in neurons of the motor cortex. All recordings were performed after a 5-minute bath application of 10 nM MLA to block $\alpha7$ nAChR responses. (A) Representative trace overlays of 10 μM ACh (red) and 1000 μM ACh (black). (B) Compilation of normalized 10–1000 μM ACh responses in the motor cortex (stippled; n = 9 neurons from six animals aged P18–P24). The ACh response to HEK cells transfected with subunit ratios to produce HS $(\alpha4)_2(\beta2)_3$ nAChRs (black) or LS $(\alpha4)_3(\beta2)_2$ nAChRs (white) are included for comparison. A 5-minute ISI was used between exposures to ACh to mitigate any possible effects of desensitization.

cortex homogenates were first immunoprecipitated with mAb290, a $\beta 2$ nAChR-selective antibody that was previously described as conformationally selective for fully assembled nAChRs (Sallette et al., 2005), then probed with both $\alpha 4$ and $\beta 2$ antibodies by Western blot (Supplemental Fig. 2). Ratios of the $\beta 2/\alpha 4$ band intensities were calculated and compared with ratios of the $\beta 2/\alpha 4$ band intensities in our surface-isolated LS and HS nAChRs in HEK cells presented in Supplemental Fig. 2B. These data support the predominance of the LS subtype in cortical homogenates.

Discussion

This study reveals that the majority of $\alpha 4\beta 2$ nAChRs examined in layers I–IV of the motor cortex are of the LS subtype. This was accomplished by normalizing responses of 10–1000 μM ACh, a paradigm that was first validated in nonlinked rat $\alpha 4\beta 2$ nAChRs. Translating receptor pharmacology from heterologous systems to ex vivo preparations involves inherent assumptions. Substantial evidence, including reporter mutations (Moroni et al., 2006), $\alpha 4/\beta 2$ transfection ratios, and concatemers (Harpsøe et al., 2011), supports the assumption that assembly of heterologously expressed $\alpha 4\beta 2$ nAChRs is limited to $(\alpha 4)_3(\beta 2)_2$ or $(\alpha 4)_2(\beta 2)_3$, rather than alternate conformations such as $(\alpha 4)_4(\beta 2)_1$ or $(\alpha 4)_1(\beta 2)_4$. Whether native receptors are restricted to these conformations is uncertain but seems likely.

Our data demonstrate that the ratio of $\alpha 4/\beta 2$ subunits in the HS subtype is opposite of that in the LS subtype (Fig. 1), confirming previous studies (Nelson et al., 2003; Moroni et al., 2006; Harpsøe et al., 2011). In addition, our functional results demonstrate a clear shift in sensitivity to activation by ACh. Moreover, the EC_{50} values (Fig. 2A) are similar to those for human HS and LS receptors (Buisson and Bertrand, 2001; Nelson et al., 2003; Moroni et al., 2006; Harpsøe et al., 2011;

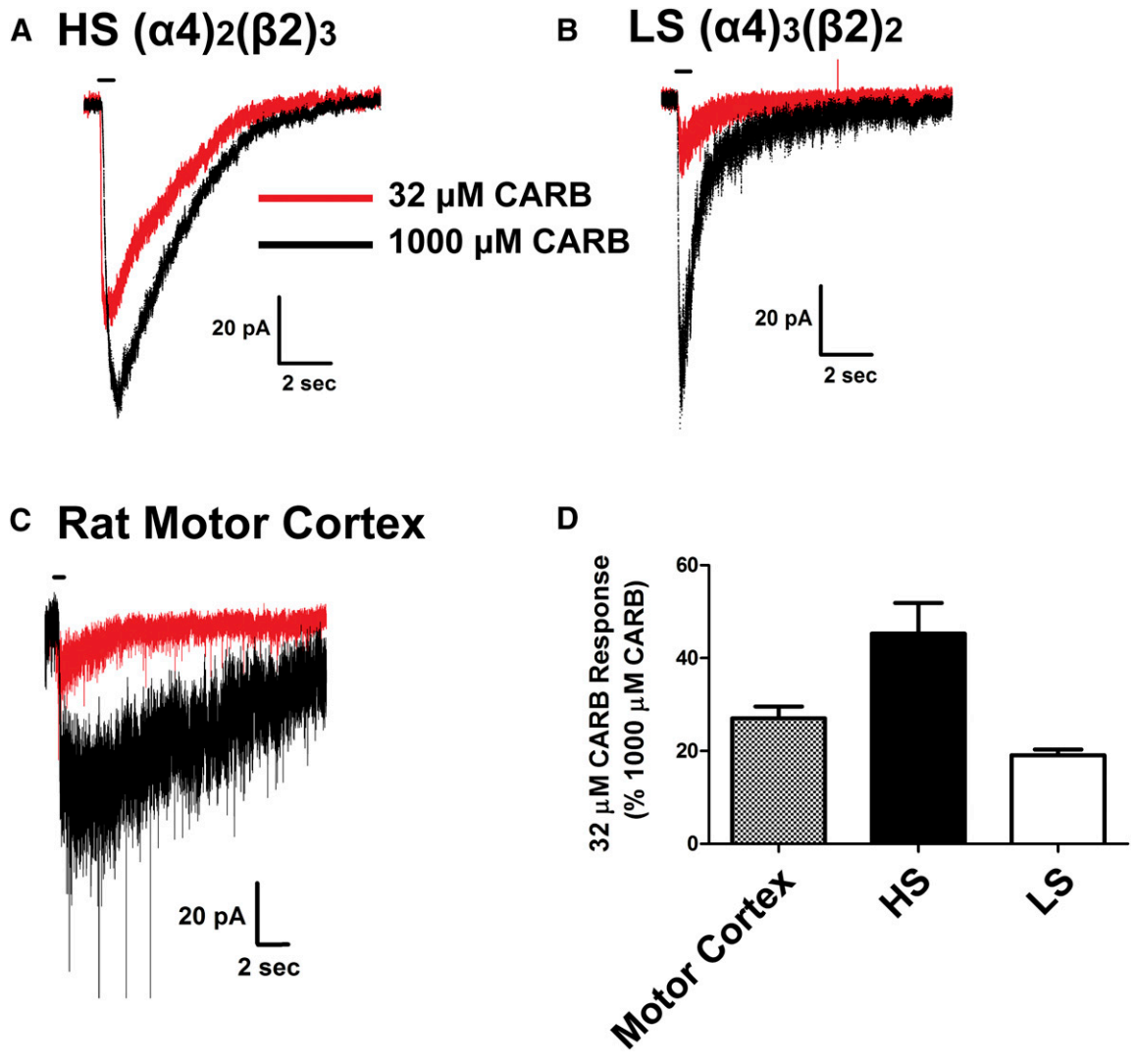

Fig. 7. Comparison of the responses to 32 and 1000 μM CARB in HS and LS HEK cells and neurons of the motor cortex. (A and B) Representative trace overlays of 32 μM CARB (red) and 1000 μM CARB (black) in HS (A) and LS (B) $\alpha 4\beta 2$ nAChRs in transfected HEK cells ($n = 4$ each transfection ratio). (C) Representative trace overlays of 32 μM CARB (red) and 1000 μM CARB (black) in the motor cortex neurons ($n = 5$ neurons from five animals aged P18–P24). (D) Quantification of 32 and 1000 μM CARB in rat motor cortex neurons (stippled). The CARB response to HEK cells transfected with subunit ratios to produce HS (black) or LS nAChRs (white) are included for comparison. All recordings were performed after a 5-minute bath application of 10 nM MLA to block $\alpha 7$ nAChR responses (neurons only) and 1 μM atropine to eliminate effects from activation of muscarinic receptors. A 5-minute ISI was used between exposures to CARB to mitigate any possible effects of desensitization.

Mazzaferro et al., 2011; Nichols et al., 2014). The ACh concentration-response curves for both transfection ratios statistically fit best to one class of receptor. However, after transfection with the 4:1 ratio, the Hill slope was 0.61 ± 0.18. Conflicting modeling of ACh dose-response curves at LS receptors has been reported (Moroni et al., 2006; Carbone et al., 2009; Harpsøe et al., 2011; Mazzaferro et al., 2011; Eaton et al., 2014). The most likely explanation for the low value obtained here is that the ACh stimulation of these LS receptors has two components, consistent with previous reports of biphasic ACh concentration-response curves (Nelson et al., 2003; Harpsøe et al., 2011; Mazzaferro et al., 2011). The LS component of this biphasic ACh response has been attributed to an $\alpha4/\alpha4$ agonist binding site, whereas the HS component of this response has been attributed to the canonical $\alpha4/\beta2$ binding site (Harpsøe et al., 2011).

The application of 1 μM Saz-A elicited a response of 69% and 25% of the 32 μM ACh response in rat HS and LS nAChRs, consistent with findings demonstrating greater efficacy at human HS nAChRs (Zwart et al., 2008; Eaton et al., 2014). When the response to 32 μM ACh was normalized to a calculated maximal response predicted by the ACh concentration-response curves, application of 1 μM Saz-A stimulated a response of 56% ± 13% of the maximum response at HS and 9.9% ± 2.4% at LS nAChRs. The value for our rat HS receptors differs from reports that Saz-A is nearly a full agonist in oocytes expressing a presumably pure population of human HS concatemeric nAChRs (Zwart et al., 2008; Eaton et al., 2014). Possible explanations for this difference are that others have assessed the efficacy of Saz-A at human $\alpha4\beta2$ nAChRs expressed in oocytes, whereas here we studied rat nAChRs expressed in mammalian cells. We studied the rat $\alpha4\beta2$ nAChRs to more readily allow comparison with responses in ex vivo rat brain slices. We decided to compare two doses of ACh in brain slices rather than the difference in efficacy of Saz-A to determine the presence of HS or LS receptors because Saz-A produces prolonged desensitization at $\alpha4\beta2$ nAChRs (Xiao et al., 2006; Eaton et al., 2014), which would have precluded our pharmacological confirmation of $\alpha4\beta2$-mediated responses using DHβE.

We sought to establish normalized responses to 10 and 1000 μM ACh at HS and LS nAChRs (Fig. 4). In applying this paradigm to the rat motor cortex, we found that the normalized response of 10–1000 μM ACh was 22%, indicating that a majority of the nAChRs are the LS nAChR subtype (Fig. 6). By utilizing our values for the same paradigm at the HS and LS $\alpha4\beta2$ subtypes in our transfected cells and extrapolating a theoretical value based upon different percentages of HS and LS receptors, we estimate that in the rat motor cortex LS nAChRs contribute about 76% of the response and the HS nAChRs contributes around 24% (Fig. 8A). This assumes that the 10 μM response as a percent of the 1000 μM response increases in a linear fashion as more HS receptors are present in the overall $\alpha4\beta2$ nAChR population.

We used the agonist CARB to corroborate the two-dose ACh paradigm. Since all of our experiments were done in the presence of 1 μM atropine to block possible signaling resulting from activation of muscarinic receptors, we only observed the nicotinic cholinergic agonist effects. Importantly, although endogenous cholinesterase activity in brain slices could alter the ACh responses in the motor cortex, CARB is not hydrolyzable by cholinesterases (Brown and Laiken, 2011). From our experiments with CARB (Fig. 7), we estimate that LS nAChRs contribute approximately 70% of the response in the rat motor cortex (Fig. 8B); thus, confirming the findings obtained using our ACh paradigm and indicating that any endogenous acetylcholinesterase activity contributes little to our results.

An immunoprecipitation and Western blot method to estimate the receptor stoichiometry also supports the conclusion of the two-concentration ACh and CARB paradigms (Supplemental Fig. 2). This experiment utilizes whole cortical homogenates rather than the motor cortex region specifically. In these biochemical experiments, about 79% of the nAChRs in rat cortex homogenates were of the LS subtype (Supplemental Fig. 2C).

One concern with the slice recordings presented here is the differential access of agonists to nAChRs on HEK cells compared with neurons due to the extracellular matrix present in slice preparations, which does not allow for instantaneous solution exchange and may impede our ability to capture accurate peak amplitude responses. This is exemplified by the delayed response and slower rise times in brain slices (Figs. 5 and 6) compared with the rapid rise times observed in HEK cells (Figs. 4 and 7). However, we were able to capture the rapid kinetics of ACh-induced $\alpha7$ nAChRs currents in brain slices using the same setup in both Fig. 5 and a previous study (Sahibzada et al., 2002). This

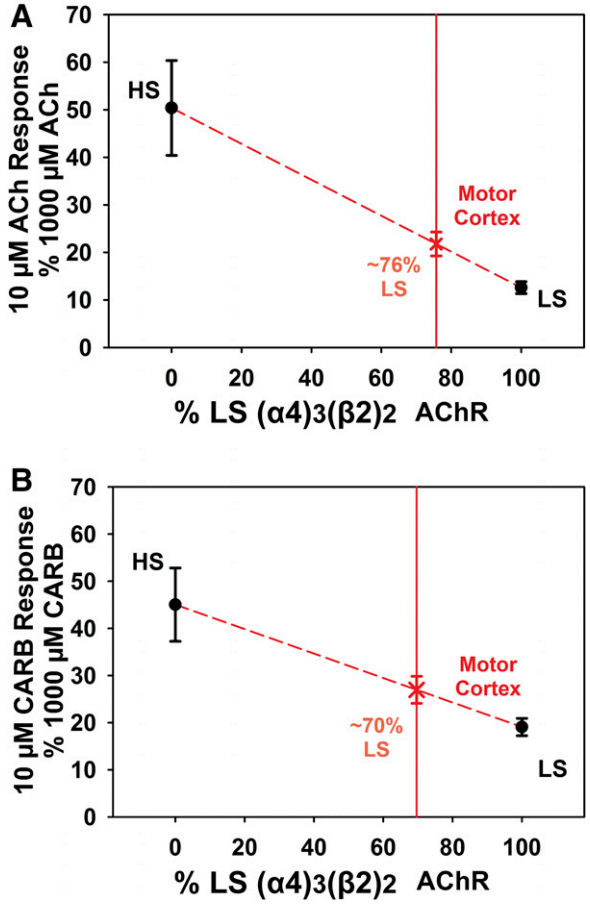

Fig. 8. Estimate of the percentage of the LS $(\alpha4)_3(\beta2)_2$ nAChR in the rat motor cortex. (A and B) On the *y*-axis, normalized 10 μM ACh (A) or 32 μM CARB (B) responses from HS and LS HEK cells are plotted against the percent contribution of LS $(\alpha4)_3(\beta2)_2$ nAChRs on the *x*-axis. Using the responses obtained from the motor cortex neuron recordings in presented in Figs. 6 and 7, we estimate that the percentage of the $\alpha4\beta2$ nAChRs in the motor cortex that are of the LS $(\alpha4)_3(\beta2)_2$ subtype is approximately 76% as determined by ACh and approximately 70% as determined by CARB.

indicates that we are likely capturing the peak amplitude response from the much slower $\alpha4\beta2$ nAChR responses. Since ACh was applied from pipettes located about 5–20 μm from the cell soma in both experiments, it is unlikely that these differential effects can be circumvented. However, in our experiments the critical interpretation is based on the ratio of responses from low and high agonist concentrations. We assume that the ratio of these two responses is independent of the degree of differential access between HEK cells and brain-slice recordings since the access in each recording scenario (i.e., HEK or slices) is similar for each pair of drug pipettes.

The possibility of channel block at higher concentrations of ACh is of concern, as it may have influenced our estimate of the ratio. However, at the high dose of ACh (1000 μM), we did not observe evidence of channel block; particularly, as there was no evidence of ensuing "hump currents" that are indicative of channel block with high doses of ACh (Liu et al., 2008). Moreover, as seen in Fig. 2A, there is a decline in the current at 3000 μM ACh, which could be due to channel block in the LS nAChRs, but this concentration is greater than the 1000 μM ACh used in our two-concentration paradigm.

Our data indicate that a majority of rat motor cortex $\alpha4\beta2$ nAChRs have lower sensitivity to ACh (EC_{50} = 56 μM versus 5 μM for HS). The difference in sensitivity to ACh probably extends to nicotine as well, since Moroni et al. (2006) found a marked difference in sensitivity to nicotine at HS versus LS $\alpha4\beta2$ nAChRs expressed in oocytes (EC_{50} = 1 μM for HS versus 34 μM for LS). In addition to the different potencies of these principal nicotinic cholinergic ligands at the two $\alpha4\beta2$ stoichiometries, some drugs such as Saz-A and A85380 (3-[(2*S*)-2-azetidinylmethoxy]-pyridine dihydrochloride) as well as nicotine demonstrate different efficacies at HS and LS nAChRs (Moroni et al., 2006; Eaton et al., 2014). For example, measured as a percentage of ACh response, nicotine has 60% efficacy at LS nAChR and only 30% efficacy at HS nAChRs (Moroni et al., 2006). The LS subtype is less sensitive to desensitization by nAChR agonists compared with the HS subtype, possibly because of the presence of the $\alpha4/\alpha4$ binding site (Benallegue et al., 2013; Eaton et al., 2014). These pharmacological differences between the HS and LS $\alpha4\beta2$ nAChRs highlight the importance of determining which of these $\alpha4\beta2$ subtypes is present and in what proportions in native tissues. This may be especially important when considering the potential use of nicotinic receptor ligands as pharmacotherapies, since accurately predicting the in vivo pharmacology of a ligand will require knowledge of receptor stoichiometry. Although the variable pharmacology and physiology between HS and LS nAChRs has been well established in heterologous expression systems, we believe this is the first determination of the relative amounts of HS and LS subtypes in the brain.

Acknowledgments

The authors thank Stefano Vicini (Georgetown University) for reviewing and making suggestions for this manuscript.

Authorship Contributions

Participated in research design: DeDominicis, Sahibzada, Xiao, Wolfe, Kellar, Yasuda.

Conducted experiments: DeDominicis, Sahibzada, Olson, Yasuda.

Contributed new reagents or analytic tools: Sahibzada, Xiao, Kellar.

Performed data analysis: DeDominicis, Sahibzada, Olson, Kellar, Yasuda.

Wrote or contributed to the writing of the manuscript: DeDominicis, Sahibzada, Wolfe, Kellar, Yasuda.

References

Alves NC, Bailey CDC, Nashmi R, and Lambe EK (2010) Developmental sex differences in nicotinic currents of prefrontal layer VI neurons in mice and rats. *PLoS One* **5**:e9261.

Anand R, Conroy WG, Schoepfer R, Whiting P, and Lindstrom J (1991) Neuronal nicotinic acetylcholine receptors expressed in Xenopus oocytes have a pentameric quaternary structure. *J Biol Chem* **266**:11192–11198.

Anderson SM and Brunzell DH (2012) Low dose nicotine and antagonism of β2 subunit containing nicotinic acetylcholine receptors have similar effects on affective behavior in mice. *PLoS One* **7**:e48665.

Anderson SM and Brunzell DH (2015) Anxiolytic-like and anxiogenic-like effects of nicotine are regulated via diverse action at β2*nicotinic acetylcholine receptors. *Br J Pharmacol* **172**:2864–2877.

Benallegue N, Mazzaferro S, Alcaino C, and Bermudez I (2013) The additional acetylcholine binding site at the α4(+)/α4(-) interface of the $(\alpha4\beta2)_2\alpha4$ nicotinic acetylcholine receptor contributes to desensitisation. *Br J Pharmacol* **170**:304–316.

Benwell MEM, Balfour DJK, and Anderson JM (1988) Evidence that tobacco smoking increases the density of (-)-[^{3}H]nicotine binding sites in human brain. *J Neurochem* **50**:1243–1247.

Brown JH and Laiken N (2011) Muscarinic receptor agonists and antagonists, in *Goodman and Gilman's The Pharmacological Basis of Therapeutics*, 12th ed (Brunton LL, Chabner BA, and Knollmann BC eds), pp 219–238, McGraw-Hill Education, New York.

Buisson B and Bertrand D (2001) Chronic exposure to nicotine upregulates the human (α)4((β)2 nicotinic acetylcholine receptor function. *J Neurosci* **21**:1819–1829.

Carbone AL, Moroni M, Groot-Kormelink PJ, and Bermudez I (2009) Pentameric concatenated $(\alpha4)_2(\beta2)_3$ and $(\alpha4)_3(\beta2)_2$ nicotinic acetylcholine receptors: subunit arrangement determines functional expression. *Br J Pharmacol* **156**:970–981.

Carignano C, Barila EP, and Spitzmaul G (2016) Analysis of neuronal nicotinic acetylcholine receptor α4β2 activation at the single-channel level. *Biochim Biophys Acta* **1858**:1964–1973.

Christophe E, Roebuck A, Staiger JF, Lavery DJ, Charpak S, and Audinat E (2002) Two types of nicotinic receptors mediate an excitation of neocortical layer I interneurons. *J Neurophysiol* **88**:1318–1327.

Eaton JB, Lucero LM, Stratton H, Chang Y, Cooper JF, Lindstrom JM, Lukas RJ, and Whiteaker P (2014) The unique α4+/-α4 agonist binding site in (α4)3(β2)2 subtype nicotinic acetylcholine receptors permits differential agonist desensitization pharmacology versus the (α4)2(β2)3 subtype. *J Pharmacol Exp Ther* **348**:46–58.

Flores CM, Dávila-García MI, Ulrich YM, and Kellar KJ (1997) Differential regulation of neuronal nicotinic receptor binding sites following chronic nicotine administration. *J Neurochem* **69**:2216–2219.

Flores CM, Rogers SW, Pabreza LA, Wolfe BB, and Kellar KJ (1992) A subtype of nicotinic cholinergic receptor in rat brain is composed of α 4 and β 2 subunits and is up-regulated by chronic nicotine treatment. *Mol Pharmacol* **41**:31–37.

Guillem K, Bloem B, Poorthuis RB, Loos M, Smit AB, Maskos U, Spijker S, and Mansvelder HD (2011) Nicotinic acetylcholine receptor β2 subunits in the medial prefrontal cortex control attention. *Science* **333**:888–891.

Harpsøe K, Ahring PK, Christensen JK, Jensen ML, Peters D, and Balle T (2011) Unraveling the high- and low-sensitivity agonist responses of nicotinic acetylcholine receptors. *J Neurosci* **31**:10759–10766.

Hussmann GP, DeDominicis KE, Turner JR, Yasuda RP, Klehm J, Forcelli PA, Xiao Y, Richardson JR, Sahibzada N, Wolfe BB, et al. (2014) Chronic sazetidine-A maintains anxiolytic effects and slower weight gain following chronic nicotine without maintaining increased density of nicotinic receptors in rodent brain. *J Neurochem* **129**:721–731.

Kassam SM, Herman PM, Goodfellow NM, Alves NC, and Lambe EK (2008) Developmental excitation of corticothalamic neurons by nicotinic acetylcholine receptors. *J Neurosci* **28**:8756–8764.

Kuryatov A, Onksen J, and Lindstrom J (2008) Roles of accessory subunits in α4β2(*) nicotinic receptors. *Mol Pharmacol* **74**:132–143.

Laemmli UK (1970) Cleavage of structural proteins during the assembly of the head of bacteriophage T4. *Nature* **227**:680–685.

Liu Q, Yu KW, Chang YC, Lukas RJ, and Wu J (2008) Agonist-induced hump current production in heterologously-expressed human α4β2-nicotinic acetylcholine receptors. *Acta Pharmacol Sin* **29**:305–319.

Lomazzo E, Hussmann GP, Wolfe BB, Yasuda RP, Perry DC, and Kellar KJ (2011) Effects of chronic nicotine on heteromeric neuronal nicotinic receptors in rat primary cultured neurons. *J Neurochem* **119**:153–164.

Lozada AF, Wang X, Gounko NV, Massey KA, Duan J, Liu Z, and Berg DK (2012) Induction of dendritic spines by β2-containing nicotinic receptors. *J Neurosci* **32**:8391–8400.

Mao D, Perry DC, Yasuda RP, Wolfe BB, and Kellar KJ (2008) The α4β2α5 nicotinic cholinergic receptor in rat brain is resistant to up-regulation by nicotine in vivo. *J Neurochem* **104**:446–456.

Marks MJ, Burch JB, and Collins AC (1983) Effects of chronic nicotine infusion on tolerance development and nicotinic receptors. *J Pharmacol Exp Ther* **226**:817–825.

Marks MJ, McClure-Begley TD, Whiteaker P, Salminen O, Brown RWB, Cooper J, Collins AC, and Lindstrom JM (2011) Increased nicotinic acetylcholine receptor protein underlies chronic nicotine-induced up-regulation of nicotinic agonist binding sites in mouse brain. *J Pharmacol Exp Ther* **337**:187–200.

Marks MJ, Meinerz NM, Drago J, and Collins AC (2007) Gene targeting demonstrates that α4 nicotinic acetylcholine receptor subunits contribute to expression of

diverse [^{3}H]epibatidine binding sites and components of biphasic $^{86}Rb^+$ efflux with high and low sensitivity to stimulation by acetylcholine. *Neuropharmacology* **53**:390–405.
Marks MJ, Pauly JR, Gross SD, Deneris ES, Hermans-Borgmeyer I, Heinemann SF, and Collins AC (1992) Nicotine binding and nicotinic receptor subunit RNA after chronic nicotine treatment. *J Neurosci* **12**:2765–2784.
Marks MJ, Whiteaker P, Calcaterra J, Stitzel JA, Bullock AE, Grady SR, Picciotto MR, Changeux JP, and Collins AC (1999) Two pharmacologically distinct components of nicotinic receptor-mediated rubidium efflux in mouse brain require the β2 subunit. *J Pharmacol Exp Ther* **289**:1090–1103.
Mazzaferro S, Benallegue N, Carbone A, Gasparri F, Vijayan R, Biggin PC, Moroni M, and Bermudez I (2011) Additional acetylcholine (ACh) binding site at α4/α4 interface of $(\alpha4\beta2)_2\alpha4$ nicotinic receptor influences agonist sensitivity. *J Biol Chem* **286**:31043–31054.
Mineur YS and Picciotto MR (2010) Nicotine receptors and depression: revisiting and revising the cholinergic hypothesis. *Trends Pharmacol Sci* **31**:580–586.
Moroni M, Zwart R, Sher E, Cassels BK, and Bermudez I (2006) α4β2 nicotinic receptors with high and low acetylcholine sensitivity: pharmacology, stoichiometry, and sensitivity to long-term exposure to nicotine. *Mol Pharmacol* **70**:755–768.
Nelson ME, Kuryatov A, Choi CH, Zhou Y, and Lindstrom J (2003) Alternate stoichiometries of α4β2 nicotinic acetylcholine receptors. *Mol Pharmacol* **63**:332–341.
Nichols WA, Henderson BJ, Yu C, Parker RL, Richards CI, Lester HA, and Miwa JM (2014) Lynx1 shifts α4β2 nicotinic receptor subunit stoichiometry by affecting assembly in the endoplasmic reticulum. *J Biol Chem* **289**:31423–31432.
Oda A, Yamagata K, Nakagomi S, Uejima H, Wiriyasermkul P, Ohgaki R, Nagamori S, Kanai Y, and Tanaka H (2014) Nicotine induces dendritic spine remodeling in cultured hippocampal neurons. *J Neurochem* **128**:246–255.
Paolone G, Angelakos CC, Meyer PJ, Robinson TE, and Sarter M (2013) Cholinergic control over attention in rats prone to attribute incentive salience to reward cues. *J Neurosci* **33**:8321–8335.
Perry DC, Dávila-García MI, Stockmeier CA, and Kellar KJ (1999) Increased nicotinic receptors in brains from smokers: membrane binding and autoradiography studies. *J Pharmacol Exp Ther* **289**:1545–1552.
Perry DC, Mao D, Gold AB, McIntosh JM, Pezzullo JC, and Kellar KJ (2007) Chronic nicotine differentially regulates α6- and β3-containing nicotinic cholinergic receptors in rat brain. *J Pharmacol Exp Ther* **322**:306–315.
Picciotto MR, Zoli M, Léna C, Bessis A, Lallemand Y, Le Novère N, Vincent P, Pich EM, Brûlet P, and Changeux J-P (1995) Abnormal avoidance learning in mice lacking functional high-affinity nicotine receptor in the brain. *Nature* **374**:65–67.
Poorthuis RB, Bloem B, Verhoog MB, and Mansvelder HD (2013) Layer-specific interference with cholinergic signaling in the prefrontal cortex by smoking concentrations of nicotine. *J Neurosci* **33**:4843–4853.
Porter JT, Cauli B, Tsuzuki K, Lambolez B, Rossier J, and Audinat E (1999) Selective excitation of subtypes of neocortical interneurons by nicotinic receptors. *J Neurosci* **19**:5228–5235.
Sahibzada N, Ferreira M, Jr, Williams B, Wasserman A, Vicini S, and Gillis RA (2002) Nicotinic ACh receptor subtypes on gastrointestinally projecting neurones in the dorsal motor vagal nucleus of the rat. *J Physiol* **545**:1007–1016.
Sallette J, Pons S, Devillers-Thiery A, Soudant M, Prado de Carvalho L, Changeux JP, and Corringer PJ (2005) Nicotine upregulates its own receptors through enhanced intracellular maturation. *Neuron* **46**:595–607.
Schwartz RD and Kellar KJ (1983) Nicotinic cholinergic receptor binding sites in the brain: regulation in vivo. *Science* **220**:214–216.
Staley JK, Krishnan-Sarin S, Cosgrove KP, Krantzler E, Frohlich E, Perry E, Dubin JA, Estok K, Brenner E, Baldwin RM, et al. (2006) Human tobacco smokers in early abstinence have higher levels of β2* nicotinic acetylcholine receptors than nonsmokers. *J Neurosci* **26**:8707–8714.
Tapia L, Kuryatov A, and Lindstrom J (2007) Ca^{2+} permeability of the $(\alpha4)_3(\beta2)_2$ stoichiometry greatly exceeds that of $(\alpha4)_2(\beta2)_3$ human acetylcholine receptors. *Mol Pharmacol* **71**:769–776.
Turner JR, Castellano LM, and Blendy JA (2010) Nicotinic partial agonists varenicline and sazetidine-A have differential effects on affective behavior. *J Pharmacol Exp Ther* **334**:665–672.
Wada E, McKinnon D, Heinemann S, Patrick J, and Swanson LW (1990) The distribution of mRNA encoded by a new member of the neuronal nicotinic acetylcholine receptor gene family (α5) in the rat central nervous system. *Brain Research* **526**:45–53.
Wang J, Kuryatov A, Sriram A, Jin Z, Kamenecka TM, Kenny PJ, and Lindstrom J (2015) An accessory agonist binding site promotes activation of α4β2* nicotinic acetylcholine receptors. *J Biol Chem* **290**:13907–13918.
Whiting P and Lindstrom J (1987) Purification and characterization of a nicotinic acetylcholine receptor from rat brain. *Proc Natl Acad Sci USA* **84**:595–599.
Wüllner U, Gündisch D, Herzog H, Minnerop M, Joe A, Warnecke M, Jessen F, Schütz C, Reinhardt M, Eschner W, et al. (2008) Smoking upregulates α4β2* nicotinic acetylcholine receptors in the human brain. *Neurosci Lett* **430**: 34–37.
Xiao C, Nashmi R, McKinney S, Cai H, McIntosh JM, and Lester HA (2009) Chronic nicotine selectively enhances α4β2* nicotinic acetylcholine receptors in the nigrostriatal dopamine pathway. *J Neurosci* **29**:12428–12439.
Xiao Y, Fan H, Musachio JL, Wei ZL, Chellappan SK, Kozikowski AP, and Kellar KJ (2006) Sazetidine-A, a novel ligand that desensitizes α4β2 nicotinic acetylcholine receptors without activating them. *Mol Pharmacol* **70**:1454–1460.
Xiao Y and Kellar KJ (2004) The comparative pharmacology and up-regulation of rat neuronal nicotinic receptor subtype binding sites stably expressed in transfected mammalian cells. *J Pharmacol Exp Ther* **310**:98–107.
Yeh JJ, Yasuda RP, Dávila-García MI, Xiao Y, Ebert S, Gupta T, Kellar KJ, and Wolfe BB (2001) Neuronal nicotinic acetylcholine receptor α3 subunit protein in rat brain and sympathetic ganglion measured using a subunit-specific antibody: regional and ontogenic expression. *J Neurochem* **77**:336–346.
Zwart R, Carbone AL, Moroni M, Bermudez I, Mogg AJ, Folly EA, Broad LM, Williams AC, Zhang D, Ding C, et al. (2008) Sazetidine-A is a potent and selective agonist at native and recombinant α 4 β 2 nicotinic acetylcholine receptors. *Mol Pharmacol* **73**:1838–1843.
Zwart R and Vijverberg HPM (1998) Four pharmacologically distinct subtypes of α4β2 nicotinic acetylcholine receptor expressed in Xenopus laevis oocytes. *Mol Pharmacol* **54**:1124–1131.

Address correspondence to: Robert P. Yasuda, Department of Pharmacology and Physiology, Georgetown University Medical Center, 3900 Reservoir Road NW, Washington, DC 20057. E-mail: yasudar@georgetown.edu; or Kenneth J. Kellar, Department of Pharmacology and Physiology, Georgetown University Medical Center, 3900 Reservoir Road NW, Washington, DC 20057. E-mail: kellark@georgetown.edu